

# Transient Sensitivity of Sectorial Split-Drain Magnetic Field-Effect Transistor

Zhenyi Yang<sup>1</sup>, Sik-Lam Siu<sup>2,4</sup>, Wing-Shan Tam<sup>2</sup>, Chi-Wah Kok<sup>2</sup>, Chi-Wah Leung<sup>3</sup>, P. T. Lai<sup>1</sup>, Hei Wong<sup>4</sup>, and P. W. T. Pong<sup>1</sup>

<sup>1</sup>Department of Electrical and Electronic Engineering, The University of Hong Kong, Hong Kong

<sup>2</sup>Canaan Semiconductor Limited, Shatin, N.T., Hong Kong

<sup>3</sup>Department of Applied Physics, The Hong Kong Polytechnic University, Hung Hom, Kowloon, Hong Kong

<sup>4</sup>Department of Electronic Engineering, City University of Hong Kong, Kowloon, Hong Kong

**This paper proposed an analytical model on the geometric dependence of the transient sensitivity and transient sensing hysteresis of sectorial split-drain magnetic field-effect transistors (SD-MAGFETs). We also conjectured that the transient sensing hysteresis is caused by the charge trapped on channel boundary, and is also geometric dependent. Experimental results are presented which show good consistence with the analytical derivation. The derived analytical model and experimental results can be used as a design guideline for the optimization and trade-off of the transient sensitivity and transient sensing hysteresis of the sectorial SD-MAGFETs.**

*Index Terms*—Hysteresis, magnetic field-effect transistor (MAGFET), sectorial, sensitivity, split-drain, transient sensitivity.

## I. INTRODUCTION

NOWADAYS, magnetic sensors find a vast range of applications in everyday lives, such as non-contact switches, positional sensors, etc. [1]–[3]. The sensing element can be realized by using different magnetic materials or by different electrical means. Recently, split-drain magnetic field-effect transistors (SD-MAGFETs) have shown to be a promising candidate as the magnetic sensing element because of its compatibility to standard CMOS process and compact-in-size [1]. The SD-MAGFETs have been fabricated in different shapes and the sectorial SD-MAGFETs were found to be able to achieve a higher sensitivity [3], [4]. Extensive research have been devoted to investigate and model the magnetic sensitivity, noise immunity, and geometric dependence for the sectorial SD-MAGFETs [3], [6], and circular SD-MAGFETs [4]. When a properly biased SD-MAGFET is placed under an external magnetic field, the Lorentz force acts on electrons moving in the channel. Consequently, a magnetic induction causes the current in the channel region to deflect up or down, depending on the direction of the magnetic field. This leads to an asymmetry in the terminal drain currents, which is a measure of the magnetic field strength. Note that the imbalance current between the two drains is a function of the transistor channel width, channel length, biasing voltages, drain source voltages, external magnetic field strength, and sector angle, etc. [4], [6]. However, it is observed that the imbalance current also exhibits a magnetic sensing hysteresis property which cannot be explained by the above external factors alone [7].

The definition of magnetic sensing hysteresis is ambiguous in literature. A formal definition is only available for magnetic sensor structured as a switch, which is constructed with an additional detection stage that compares the different outputs of the MAGFET to a chosen voltage/current. As a result, the detection stage will output a logic high when the magnetic field induced voltage/current difference measured at the output of the MAGFET is larger than the chosen value. Otherwise,

it will output a logic low. If the MAGFET has sensing hysteresis, the magnetic field strength that will induce the desired voltage/current will be different at increasing and decreasing magnetic field strength. It is our objective in this paper to investigate the magnetic sensing hysteresis property of the sectorial SD-MAGFET. In particular, we shall focus our investigation on the difference in the magnetic response under increasing and decreasing magnetic field strength in general without the detection stage. The understanding of the SD-MAGFET sensing hysteresis is important both theoretically and practically. Similar to other sensing and detection applications, the sensing hysteresis property can be applied to promote noise immunity of the sensing and detection process, which in turn helps to avoid false detection, and noise triggering similar to the Schmitt-trigger in digital circuitry. Previous works on magnetic sensor with field-effect transistor structure [8], [9] have shown that the sensing hysteresis can be caused by holes in the channels, where the holes are caused by faulty interface between the ferromagnetic field (In, Mn), and the silicon. In this work, we conjecture that the channel boundary charge trapping in pure CMOS MAGFET will also cause sensing hysteresis. Therefore, we developed an analytical model of the magnetic sensitivity of sectorial SD-MAGFET with and without channel boundary charge trapping effects. We shall also consider the geometric effect of the sectorial SD-MAGFET on sensitivity, which helps to reveal the fact that the sensitivity and also the intensity of sensing hysteresis are geometry dependent. The sensitivity model and also sensing hysteresis model of sectorial SD-MAGFET to be derived from this study can be applied to design the sectorial SD-MAGFET based magnetic sensor with the desired property without tedious post-fabrication device tuning step.

## II. CHANNEL CHARGE TRAPPING AND SENSITIVITY HYSTERESIS MODEL OF SD-MAGFET

The layout of a N-Channel sectorial SD-MAGFET studied in this paper is shown in Fig. 1, which consists of a source terminal (Source) and two drain terminals (Drain 1 and Drain 2). Note that the gray contrast are used to identify the channel area and the source/drain areas in the SD-MAGFET. The radius of the source terminal, the channel length, the channel width between the source and the drain terminals, the spacing between the two drain terminals, the drain channel overlap, and the angle sustained by the sectorial SD-MAGFET are denoted

Manuscript received November 05, 2012; revised December 25, 2012; accepted January 11, 2013. Date of current version July 15, 2013. Corresponding author: P. W. T. Pong (e-mail: ppong@eee.hku.hk).

Color versions of one or more of the figures in this paper are available online at <http://ieeexplore.ieee.org>.

Digital Object Identifier 10.1109/TMAG.2013.2241034

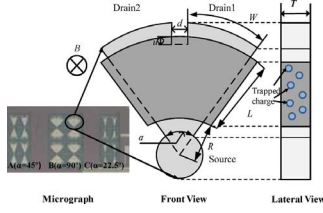


Fig. 1. Structure of the SD-MAGFETs. The front and lateral view of the layout of the sectorial SD-MAGFET with sector angle  $\alpha$ , channel length  $L$ , channel width  $W$ , source radius  $R$ , drain separation  $d$ , and drain channel overlapping  $u$ , where the source/drain region and channel region are in light gray and dark gray, respectively. The magnetic field is perpendicular to the SD-MAGFET channel. The micrograph of the fabricated SD-MAGFETs in 2.25  $\mu\text{m}$  metal gate process is shown in the bottom left corner with samples A, B, and C.

as  $R$ ,  $L$ ,  $W$ ,  $d$ ,  $u$ , and  $\alpha$ , respectively. A magnetic field  $B$  is applied perpendicular to the channel (as indicated by the marker in Fig. 1). The magnetic field strength will induce a Lorentz force that deflects the electrons in the channel from Drain 1 to Drain 2, and thus creates a differential current known as the Hall current [1] given by  $\Delta I_H = I_{DS1} - I_{DS2}$ , where  $I_{DS1}$  and  $I_{DS2}$  are the drain currents measured at Drain 1 and Drain 2, respectively. Therefore, the sensitivity of the SD-MAGFET under the applied magnetic field strength is given by [1]

$$S = \frac{1}{I_{DS}} \times \frac{\Delta I_H}{B}. \quad (1)$$

Follow the derivation in [3], [4], the Hall current is given by

$$\Delta I_H = \frac{\mu_H B I_{DS1,0} \ln\left(\frac{L+R}{R}\right)}{\alpha + \epsilon_1}, \quad (2)$$

where  $I_{DS1,0}$  is the current of the SD-MAGFET without B-field with the SD-MAGFET biased at saturation, and thus  $I_{DS1,0}$  depends on both  $V_{GS}$  and the SD-MAGFET threshold voltage  $V_{th}$ . The variable  $\epsilon_1$  is introduced to account for the geometric approximation error of the conversion between rectangular SD-MAGFET and sectorial SD-MAGFET. As a result, the two drain currents will be given by

$$I_{DS1} = I_{DS1,0} + \Delta I_H/2 = I_{DS1,0}(1 + K_1), \quad (3)$$

$$I_{DS2} = I_{DS2,0} - \Delta I_H/2 = I_{DS1,0}(1 - K_1), \quad (4)$$

where  $K_1 = (\mu_H B \ln((L+R)/(R)))/(2(\alpha + \epsilon_1))$ . Note that  $I_{DS2,0}$  is the current at Drain 2 of the SD-MAGFET without magnetic field. Finally, the magnetic sensitivity of the sectorial SD-MAGFET is given by

$$\begin{aligned} S &= \frac{\Delta I_H}{I_{DS} B} = \frac{2I_{DS1,0} K_1}{I_{DS1,0} B} \\ &= \frac{2K_1}{B} = \frac{\mu_H \ln\left(\frac{L+R}{R}\right)}{\alpha + \epsilon_1}. \end{aligned} \quad (5)$$

It is vivid from (5) that  $S$  is inversely proportional to  $\alpha$  with

$$\frac{1}{S} = m_1 \alpha + m_0. \quad (6)$$

Consider the case when there are trapped charges at the channel boundary as depicted in Fig. 1, the trapped charges affect the Lorentz force and hence the current density in the drains varies. Our experimental observation of the temporary sensing hysteresis suggests a low energy transient charge trap, where the charge trapping density on the channel boundary depends on the probability of charges reaching the channel boundary, and is therefore modeled to be inversely proportion to  $\alpha$ . As a result,

TABLE I  
GEOMETRIC PARAMETERS OF THE SD-MAGFETS

Sample No.	A	B	C
Channel length $L$ ( $\mu\text{m}$ )	49	49	49
Radius of source $R$ ( $\mu\text{m}$ )	10	10	10
Sector angle $\alpha$ (degree)	45	90	22.5
Drain separation $d$ ( $\mu\text{m}$ )	3	3	3
Drain channel overlap $u$ ( $\mu\text{m}$ )	1	1	1

the induced Hall current of the sectorial SD-MAGFET under magnetic field  $B$  with the influence of trapped charges on the channel boundary is given by

$$\Delta \hat{I}_H = \frac{\mu_H B I_{DS1,0} \ln\left(\frac{L+R}{R}\right) A}{(\alpha + \hat{\epsilon}_1)(\alpha + \hat{\epsilon}_2)}, \quad (7)$$

where  $A$  is the proportional variable that accounts for the boundary charge trapping effect, the  $V_{GS}$ , and other geometric factors besides  $L$ ,  $R$ , and  $\alpha$ . However, if we will only consider a single biasing voltage  $V_{GS}$ , and keep other geometric factors to be the same,  $A$  can be considered to be a constant. The variables  $\hat{\epsilon}_1$  and  $\hat{\epsilon}_2$  account for the geometric approximation errors in SD-MAGFET geometric conversion and using  $\alpha$  to approximate the charge trapping density, respectively. Hence, the magnetic sensitivity  $S_T$  of the sectorial SD-MAGFET under the effect of channel boundary charge trapping is given by

$$S_T = \frac{\Delta \hat{I}_H}{I_{DS1,0} B} = \frac{A \mu_H \ln\left(\frac{L+R}{R}\right)}{(\alpha^2 + (\hat{\epsilon}_1 + \hat{\epsilon}_2)\alpha + \hat{\epsilon}_1 \hat{\epsilon}_2)}, \quad (8)$$

which is inversely proportion to a quadratic function of  $\alpha$ , such that

$$\frac{1}{S_T} = \hat{m}_2 \alpha^2 + \hat{m}_1 \alpha + \hat{m}_0. \quad (9)$$

Equations (6) and (9) have shown that the magnetic sensitivity of sectorial SD-MAGFET without and with the effect of boundary charge trapping effect is inversely proportional to  $\alpha$  and a quadratic function of  $\alpha$ , respectively. In other words, it is geometric dependent. The following section will present experimental results which are shown to be consistent with the above derived analytical model.

### III. EXPERIMENTS

To investigate the transient sensitivity of the sectorial SD-MAGFET with different  $\alpha$  under the effect of charge trapping at channel boundary, three samples with different geometric parameters were fabricated using a commercial 2.25  $\mu\text{m}$  Metal Gate CMOS process provided by Founder Microelectronics International Corp. Ltd., where the micrograph of the fabricated devices are shown in Fig. 1. To mitigate the adverse effect of layout mismatch and measurement noise, eight sectorial SD-MAGFETs with the same geometric parameters as listed in Table I were cross-couple connected to form an equivalent sectorial SD-MAGFET. Such that the measured  $\Delta I_H$  will be larger than the minimum measurement limit. With eight sectorial SD-MAGFET connected in parallel, the  $\Delta I_H$  induced by a given B-field strength will be eight times larger than that of a single device. The channel lengths of the three samples are the same whereas their channel width varies with varying  $\alpha$ . Fig. 2 shows the characterization circuit for the sectorial SD-MAGFET in this experiment, which consists of a pair of off-chip resistors  $R_1$  and  $R_2$  connecting to Drain 1 and Drain 2 of the sectorial SD-MAGFET, respectively. The resistance of  $R_1$  and  $R_2$  are chosen to be larger than 100  $\text{K}\Omega$ , such that large enough voltage difference is induced by  $\Delta I_H$ . The  $R_1$

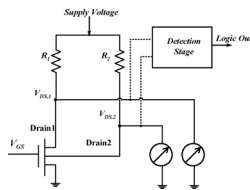


Fig. 2. Characterization circuit of the sectorial SD-MAGFET, which consists of a set of off-chip balancing resistors ( $R_1$  and  $R_2$ ).

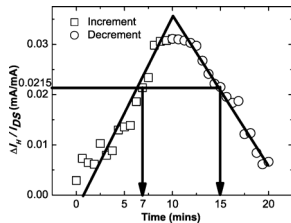


Fig. 3. Plot of  $\Delta I_H/I_{DS}$  as a function of time where the magnetic field varies from 0 T to 0.8 T from 0 mins to 10 mins linearly, and then from 0.8 T to 0 T from 10 mins to 20 mins linearly. The device under measured has  $\alpha = 90^\circ$ .

and  $R_2$  are further chosen to compensate the layout mismatch problem of the sectorial SD-MAGFET, such that sufficient perturbation on the resistance of  $R_1$  and  $R_2$  are provided to achieve zero differential voltage to be measured on the drains of the sectorial SD-MAGFET when it is not exposed to any external magnetic field. A supply voltage of 2.7 V and a gate voltage of 1.4 V were applied to bias the SD-MAGFET to work in saturation mode at room temperature ( $25^\circ\text{C}$ ). Experimental results showed that  $\Delta I_H$  will reduce dramatically with  $V_{GS}$  smaller than 1.4 V. While only very small increment in  $\Delta I_H$  is observed with  $V_{GS}$  greater than 1.4 V. This observation is consistent with the MOSFET biased at saturation. Therefore, we shall consider  $V_{GS}$  equals 1.4 V in all of the following experiments.

The magnetic sensitivity of the sectorial SD-MAGFETs under increasing and decreasing magnetic field strength were measured by inducing a magnetic field that is perpendicular to the channel of the sectorial SD-MAGFET using the Lake Shore 7400 Series Vibrating Sample Magnetometer. A uniform magnetic field is believed to be applied to the MAGFET because of the very large surface area of the electro-magnet compared to the size of the MAGFET. The voltage variation of  $V_{DS1}$  and  $V_{DS2}$  are measured by using the Digital Multimeter MS8200G. By subtracting  $V_{DS1}$  and  $V_{DS2}$  from the supply voltage and divide the results by the resistance of  $R_1$  and  $R_2$ , respectively, we shall obtain  $I_{DS1}$  and  $I_{DS2}$ . The  $V_{DS}$  are measured under a consecutive increasing magnetic field varied from 0 T to 0.3 T and then a decreasing magnetic field from 0.3 T to 0 T for Sample A ( $\alpha = 45^\circ$ ) and Sample C ( $\alpha = 22.5^\circ$ ), and from 0 T to 0.8 T and then from 0.8 T to 0 T for Sample B ( $\alpha = 90^\circ$ ), where the time for each field sweeping cycle is 10 minutes for the increasing field and 10 minutes for the decreasing field strength. The particular choice of 10 minutes increasing magnetic field strength and 10 minutes decreasing magnetic field strength is based on the decision to investigate the SD-MAGFET sensitivity with and without the influence of fully filled channel boundary charge traps.

#### IV. RESULTS AND DISCUSSION

An example of the measured  $\Delta I_H/I_{DS}$  as a function of time of samples with angle  $\alpha = 90^\circ$ ,  $R = 10 \mu\text{m}$  and  $L = 49 \mu\text{m}$  is plotted in Fig. 3, where the magnetic field varies from 0 T to 0.8 T from 0 mins to 10 mins linearly, and then from

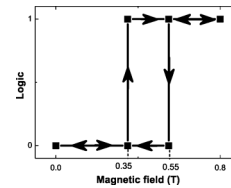


Fig. 4. Logic output of the magnetic switch with the detector connected in Fig. 2 for the sectorial SD-MAGFET with measurement results in Fig. 3.

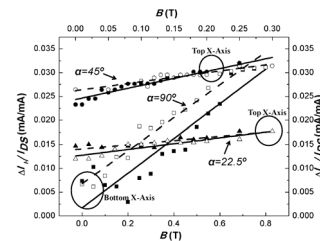


Fig. 5. Plot of  $\Delta I_H/I_{DS}$  as a function of magnetic field for samples A, B and C while the black markers and the white markers represent the experimental data for increasing and decreasing magnetic field strength, respectively. The solid line and the dashed line are the fitted curves for increasing and decreasing magnetic field strength, respectively.

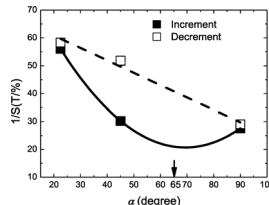


Fig. 6. Plot of inverse sensitivity curves as a function of sector angle  $\alpha$  under increasing (the solid line) and decreasing (the dashed line) magnetic field, where the markers are the experimental data and the curves are the analytical model. The best sensitivity of the sectorial SD-MAGFET under increasing magnetic field strength is observed at  $\alpha = 65^\circ$ .

0.8 T to 0 T from 10 mins to 10 mins linearly. Since the sensitivity is linearly proportional to  $\Delta I_H/I_{DS}$ , it is vivid from the slope of the plotted measurement results that the device has different sensitivity in the increasing and decreasing magnetic field strength. The magnetic switch formed by this sectorial SD-MAGFET by connecting a detector to the two drains of the MAGFET, as shown by the dotted line in Fig. 2, will generate a logical output as shown in Fig. 4, where the detection is at  $\Delta I_H/I_{DS} = 0.0215$ . It can be observed from Fig. 4 that the difference in transient sensitivity of the sectorial SD-MAGFET in the increasing and decreasing magnetic field strength will lead to a magnetic switch hysteresis.

Fig. 5 has plotted the measurement results of  $\Delta I_H/I_{DS}$  as a function of  $B$  for samples with different  $\alpha$ , where the black and white markers represent the experimental data obtained from increasing and decreasing magnetic field strength, respectively. A set of linearly fitted curves from the experimental data are shown on the same figure, where the slope of the curves represents the sensitivity of the sectorial SD-MAGFET as depicted in (1). The sensitivity of the sectorial SD-MAGFET is observed to be linearly proportional to the magnetic field strength, for both increasing and decreasing in magnetic field strength.

Fig. 6 shows the plots of  $1/S$  as a function of  $\alpha$  with increasing (the solid line and black markers) and decreasing (the dashed line and white markers) magnetic field strength. It can be observed that  $1/S$  is quadratically related to  $\alpha$  (the solid line) under increasing magnetic field strength. On the other hand, the  $1/S$  is observed to be linearly related to  $\alpha$  (the dashed line) under decreasing magnetic field strength. These

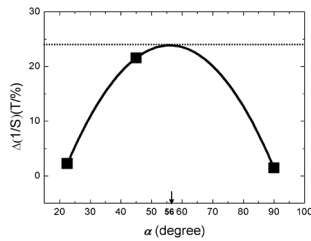


Fig. 7. Plot of the  $\Delta(1/S) = 1/S - 1/S_T$  as a function of sector angle  $\alpha$ , with  $1/S$  and  $1/S_T$  curves for decreasing and increasing magnetic field strength respectively in Fig. 6, where the maximum difference is observed at  $\alpha = 56^\circ$ .

curves for increasing and decreasing magnetic strength field are well matched with the expression depicted in (9) and (6), respectively, with added proportional constants which accounts for the difference between reality and the assumptions of perfectly fabricated sectorial SD-MAGFET and imperfect measurement equipment used in the experiment. The coefficients of both equations fitted to the obtained experimental results are  $m_1 = -0.4438$ ,  $m_0 = 69.6893$ ,  $\hat{m}_2 = 0.0161$ ,  $\hat{m}_1 = -2.2335$  and  $\hat{m}_0 = 98.1553$  respectively ( $m_1$  is negative in value because B-field has to be negative in order to satisfy the current condition listed in (3) and (4)). It shows that the sectorial SD-MAGFET has been influenced by the charge trapped at channel boundary only under the case of increasing magnetic field strength. This can be attributed to the low energy trapping at the channel boundary where the trapped charge can only be sustained by applying an additional electric field induced by increasing Lorentz force. The best sensitivity of the sectorial SD-MAGFET under increasing magnetic field strength is observed at  $\alpha = 65^\circ$  where  $1/S$  attains its minimal value as shown in Fig. 6. This result is consistent with that presented in [3], [6], and is due to the existence of the trapped charges which establishes a reverse electric field that mitigates the effect of increasing  $\alpha$ . The sensitivity of sectorial SD-MAGFET under decreasing magnetic field strength is linearly related to  $\alpha$  which is consistent with the traditional Hall-square type magnetic sensor property without the influence of channel boundary charge trapping. This is due to the declining Lorentz force under decreasing magnetic field strength, which does not provide enough charge deflection, and hence cannot refill the trap center after the charge has been escaped from the trap center. Our experiment has showed that the sectorial SD-MAGFET fabricated by the metal gate CMOS process considered this paper has a short trapped charge survival time, where the  $\Delta I_H/I_{DS}$  obtained at decreasing magnetic field strength will gradually decrease to match that of increasing magnetic field after long enough waiting (the time depends on the magnetic field strength under consideration) with the magnetic field strength maintained at constant. In other words, the observed sensing hysteresis effect is transient in nature. If the applied magnetic field strength varies faster than the charge detrapping time, we shall not be able to observe the sensing hysteresis effect, and the sectorial SD-MAGFET will be observed to have a constant sensitivity equals to that of the increasing magnetic field strength for both increasing and decreasing magnetic field strength.

The difference of  $1/S$  obtained between slow varying increasing and decreasing magnetic field strengths shows a quadratic relation with  $\alpha$  as shown in Fig. 7 which plots  $1/S - 1/S_T$  with  $1/S$  and  $1/S_T$  given by (6) and (9), respec-

tively. We conjectured that the transient sensing hysteresis of the sectorial SD-MAGFET is quadratically related to  $\alpha$ , and reaches its maximum at  $\alpha = 56^\circ$ . This is the geometric shape that provides the highest transient sensing hysteresis, which can guide a circuit designer to design a sectorial SD-MAGFET. Noted that the  $\alpha$  that achieves the best sensitivity ( $65^\circ$ ) is not the same as that achieves the highest transient sensing hysteresis ( $56^\circ$ ). This is due to the difference between the second order derivative of the  $1/S$  function and that of the difference between the  $1/S$  functions of the slow varying magnetic field. Our analytical derivation and experimental results showed that an appropriate  $\alpha$  is needed in order to obtain a satisfactory trade-off between sensitivity and transient sensing hysteresis for the sectorial SD-MAGFETs. It should also be noted that the survival time of the trapped charge depends on the electron and trap center densities and also the applied magnetic and electric fields. Thus the transient sensing hysteresis attributed to charge trapping varies with the duration of the magnetic field cycle adopted in the experiment. However, the obtained sensitivity curves do follow those obtained in Figs. 4, 6, and 7 when the variation of the magnetic field strength is slow.

## V. CONCLUSION

We derived analytical relation between the sensitivity and geometric parameters of sectorial SD-MAGFETs. We showed that without the influence of channel boundary charge trapping, the sensitivity of sectorial SD-MAGFET should be inversely proportional to the sector angle  $\alpha$ , whereas under channel boundary charge trapping, the sensitivity of sectorial SD-MAGFET is an inverse to a quadratic function of  $\alpha$ . These analytical sensitivity analysis helps to explain the transient sensing hysteresis property of the sectorial SD-MAGFET under slow varying field, and we conjectured that it is caused by charge trapped on the channel boundary. We further showed that the degree of transient hysteresis is quadratically related to the geometric factor  $\alpha$ . The experimental results show good consistency with the analytical derivation. This work not only provides an analytical model on the working principle of the sectorial SD-MAGFET but also provides the circuit designer a design guideline on how to design sectorial SD-MAGFET to achieve the best sensitivity, largest sensing hysteresis, and finally the trade-off between sensitivity and transient sensing hysteresis.

## REFERENCES

- [1] J. E. Lenz, "A review of magnetic sensors," *Proc. IEEE*, vol. 78, pp. 973–989, 1990.
- [2] S. L. Chen, C. H. Kuo, and S. I. Liu, "CMOS magnetic field to frequency converter," *IEEE Sensors J.*, vol. 3, no. 2, pp. 241–245, Apr. 2003.
- [3] Y. R. Yao, D. Z. Zhu, and Q. Guo, "Sector split-drain magnetic field effect transistor based on standard CMOS technology," *Sens. Actuat. A: Phys.*, vol. 121, no. 2, pp. 347–351, Jun. 2005.
- [4] B. W. Zhang, C. W. Korman, and M. E. Zaghoul, "Circular MAGFET design and SNR optimization for magnetic bead detection," *IEEE Trans. Magn.*, vol. 48, no. 11, pp. 3851–3854, Nov. 2012.
- [5] G. F. Santillan-Quiñonez, V. Champac, and R. S. Murphy, "Exploiting magnetic sensing capabilities of short split-drain MAGFETs," *Solid-State Electron.*, vol. 54, no. 11, pp. 1239–1245, Nov. 2010.
- [6] Q. Guo, D. Z. Zhu, and Y. R. Yao, "CMOS magnetic sensor integrated circuit with sectorial MAGFET," *Sens. Actuat. A: Phys.*, vol. 126, no. 1, pp. 154–158, Jan. 2006.
- [7] F. Ning and E. Bruun, "An offset-trimmable array of magnetic-field-sensitive MOS transistors (MAGFETs)," *Sens. Actuat. A*, vol. 58, pp. 109–112, 1997.
- [8] Y. Nishitani *et al.*, "Magnetic anisotropy in a ferromagnetic (Ga, Mn)Sb thin film," *Phys. E*, vol. 4, pp. 2681–2684, 2010.
- [9] F. Matsukura *et al.*, "Control of ferromagnetism in field-effect transistor of a magnetic semiconductor," *Phys. E*, vol. 12, pp. 351–355, 2002.